Proximal Tubular Cell–Specific Ablation of Carnitine Acetyltransferase Causes Tubular Disease and Secondary Glomerulosclerosis

Claudia Kruger,[1] Trang-Tiffany Nguyen,[1] Chelsea Breaux,[1] Alana Guillory,[1] Margaret Mangelli,[1] Kevin T. Fridianto,[2] Jean-Paul Kovalik,[2] David H. Burk,[3] Robert C. Noland,[4] Randall Mynatt,[5] and Krisztian Stadler[1]

Diabetes 2019;68:819–831 | https://doi.org/10.2337/db18-0090

Proximal tubular epithelial cells are highly energy demanding. Their energy need is covered mostly from mitochondrial fatty acid oxidation. Whether derailments in fatty acid metabolism and mitochondrial dysfunction are forerunners of tubular damage has been suggested but is not entirely clear. Here we modeled mitochondrial overload by creating mice lacking the enzyme carnitine acetyltransferase (CrAT) in the proximal tubules, thus limiting a primary mechanism to export carbons under conditions of substrate excess. Mice developed tubular disease and, interestingly, secondary glomerulosclerosis. This was accompanied by increased levels of apoptosis regulator and fibrosis markers, increased oxidative stress, and abnormal profiles of acylcarnitines and organic acids suggesting profound impairments in all major forms of nutrient metabolism. When mice with CrAT deletion were fed a high-fat diet, kidney disease was more severe and developed faster. Primary proximal tubular cells isolated from the knockout mice displayed energy deficit and impaired respiration before the onset of pathology, suggesting mitochondrial respiratory abnormalities as a potential underlying mechanism. Our findings support the hypothesis that derailments of mitochondrial energy metabolism may be causative to chronic kidney disease. Our results also suggest that tubular injury may be a primary event followed by secondary glomerulosclerosis, raising the possibility that focusing on normalizing tubular cell mitochondrial function and energy balance could be an important preventative strategy.

Although there is no doubt that glomerular disease is a major feature in the development of both diabetic nephropathy (DN) and obesity-related chronic kidney disease (CKD), evidence now also indicates proximal tubular injury as an important early event in kidney disease (1–3). Proximal tubular epithelial cells (PTCs) are highly energy demanding and contain a large number of mitochondria. Their high energy need is primarily covered from mitochondrial fatty acid oxidation to produce ATP (4–6). Excess fatty acid metabolites can be shuttled to cytoplasmic lipid droplets to shield from toxicity, but this buffer capacity is limited in PTCs (7,8). Therefore, disturbances in fatty acid oxidation appear to cause PTC atrophy through apoptosis (9–15). In type 2 diabetes and obesity, persistently elevated triglyceride and free fatty acid levels in the circulation (16) are damaging to tubular cells (17,18). Recent discoveries show that metabolic alterations in tissues affected by diabetic complications are tissue specific, with increased fatty acid metabolism in the kidney of mice and humans with type 2 diabetes (19). Increased β-oxidation, however, is not matched with ATP production. The kidney cortex (~90% tubular cells) shows accumulation of intermediate metabolic products from mitochondrial β-oxidation. After an initial increase, tricarboxylic acid (TCA) cycle activity slows in advanced kidney disease, and organic acid metabolites from the TCA cycle are lost into the urine. These conditions altogether are consistent with "mitochondrial lipid overload" (20–24).

[1]Oxidative Stress and Disease Laboratory, Pennington Biomedical Research Center, Baton Rouge, LA
[2]Programme in Cardiovascular & Metabolic Disorders, Duke-National University of Singapore (NUS) Medical School, Singapore
[3]Cell Biology and Bioimaging Core, Pennington Biomedical Research Center, Baton Rouge, LA
[4]Skeletal Muscle Metabolism Laboratory, Pennington Biomedical Research Center, Baton Rouge, LA
[5]Transgenics Core, Pennington Biomedical Research Center, Baton Rouge, LA

Corresponding author: Krisztian Stadler, krisztian.stadler@pbrc.edu

Received 19 January 2018 and accepted 28 January 2019

Mitochondrial overload is not a new phenomenon, but its contribution to CKD is not known. It was first described in skeletal muscle in the context of insulin resistance (22), where mitochondria are presented with substrate excess. This substrate excess overwhelms the catabolic capacity of mitochondrial β-oxidation. Consequently, free CoA levels decline as increased supply and oxidation of fatty acids leads to accumulation of excess acetyl-CoA. Mitochondrial overload also results in increased levels of incompletely oxidized products: long- and medium-chain acylcarnitines and acyl-CoAs. Sustained elevation in incomplete fatty acid oxidation then may foster a mitochondrial microenvironment conducive to oxidant stress (25). This is because a chronic increase in substrate entry to the mitochondria produces reducing equivalents in excess of that which can be handled by the electron transport chain (ETC). This leads to increased NADH and $FADH_2$ (reduced form of flavin adenine dinucleotide) levels. Such an increase was proposed to induce electron "backpressure" and reactive oxygen species (ROS) production.

To model this mitochondrial substrate overload, we ablated the enzyme carnitine acetyltransferase (CrAT) in proximal tubular epithelial cells in mice (PT-CrAT mice). CrAT is a mitochondrial matrix enzyme, serving as a "relief valve" (26). It facilitates the export of excess, preferably short-chain acyl-CoA products out of the mitochondria by linking them to carnitine, making these products membrane permeable (23). Because acylcarnitines can traverse membranes, CrAT also plays a key role in regulating cellular/mitochondrial acetyl- and acyl-CoA balance and carbon trafficking. In the absence of CrAT, the acetyl-CoA–to–CoA ratio increases, and some partially oxidized products cannot exit the mitochondria. CrAT deletion therefore leads to the accumulation of incompletely oxidized acyl-CoA products and mitochondrial acetyl-CoA overload (22,27).

Our goal in the current study was to understand whether such conditions can be the forerunners of tubular disease. We demonstrate that PT-CrAT mice develop not only tubular but also glomerular disease and that a high-fat diet (HFD) exacerbates pathology. We also provide evidence that impaired mitochondrial respiration in overloaded PTCs precedes the onset of disease development. Thus, our data indicate that PTC-specific deletion of CrAT causes kidney disease and that mitochondrial overload promotes the acceleration of CKD in relation to metabolic disease.

RESEARCH DESIGN AND METHODS

All animal studies were performed at the Association for Assessment and Accreditation of Laboratory Animal Care International–accredited facility of Pennington Biomedical Research Center and approved by the Institutional Animal Care and Use Committee.

Animals

Mice with targeted deletion of CrAT in the PTC were generated using the Cre-loxP recombination strategy (Fig. 1). Homozygous CrATloxP female mice (C57BL/6J) were bred to male γ-glutamyl transferase Cre mice (*Tg-(Ggt1-cre)M3Egn/J*, mixed Balb/cJ/C57BL/6 background; The Jackson Laboratory). Offspring heterozygous to CrATloxP were backcrossed to the CrATloxP mice. This cross produced offspring of which 50% were PTC-specific CrAT ablated (PT-CrAT) mice. Littermate homozygous fl/fl, Cre-negative mice were used as controls. To verify the regions of the kidney with Cre-recombinase activity, a set of PT-CrAT female mice were bread with a "tdTomato" (*B6.Cg-Gt(ROSA)26Sor<tm14(CAG-tdTomato)Hze>/J*) male.

Kidneys of the Cre-positive offspring were dissected at 4 weeks of age, sectioned, and photographed under a Leica DM6000 fluorescent microscope. Another set of kidneys from fl/fl control and PT-CrAT mice (n = 4/genotype) were harvested. One kidney per mouse was cryosectioned and stained with an anti–active-Cre antibody (1:100) (Novagen). Sections were photographed as described above. The other kidney as well as heart, skeletal muscle, and epididymal white adipose tissue were used for quantitative (q) PCR and Western blot analyses to determine CrAT mRNA expression and protein levels. CrAT activity from kidney homogenates was measured as previously described (23). Genotyping was performed on tail DNA using standard PCR reagents.

Mice were kept in a room with a 12/12-h light/dark cycle and had access to food and water ad libitum. Mice were randomly divided into cohorts and fed a chow diet (5001 Purina Rodent Chow) for 6, 12, 15, 18, and 24 months. Other cohorts were fed a low-fat diet (LFD) (10% kcal fat from lard) (D12450B; Research Diets) or an HFD (60% kcal fat from lard) (D12492) up to 18 months. At the end of each time point, mice were placed in a metabolic chamber for a 24-h acclimation. Urine was collected every 24 h, and the 72-h urine was used for proteinuria analysis and mass spectrometry. Fasting blood glucose levels were measured from a drop of blood from the tail vein (OneTouch). For glucose tolerance test, mice received a dose of 10% glucose solution (200 μL/50 g body wt, i.p.), and blood glucose levels were measured at 30, 60, 90, and 120 min. Kidneys were excised and halved. One kidney was fixed in 4% paraformaldehyde and processed for paraffin embedding, and the other kidney was processed in optimal cutting temperature media for cryocutting and immunofluorescent staining.

Histology

Paraffin-embedded kidneys were cut into 5-μm cross sections. Sections were mounted on charged Superfrost slides (Fisher Scientific) and deparaffinized. Sections were stained with *1*) periodic acid–Schiff (PAS) to evaluate glomerular size, sclerosis, and proteinaceous casts and with *2*) trichrome for fibrosis and collagen deposits. At least 10 viewing areas per slide were evaluated on each section with a NanoZoomer Digital Pathology Virtual Slide Viewer.

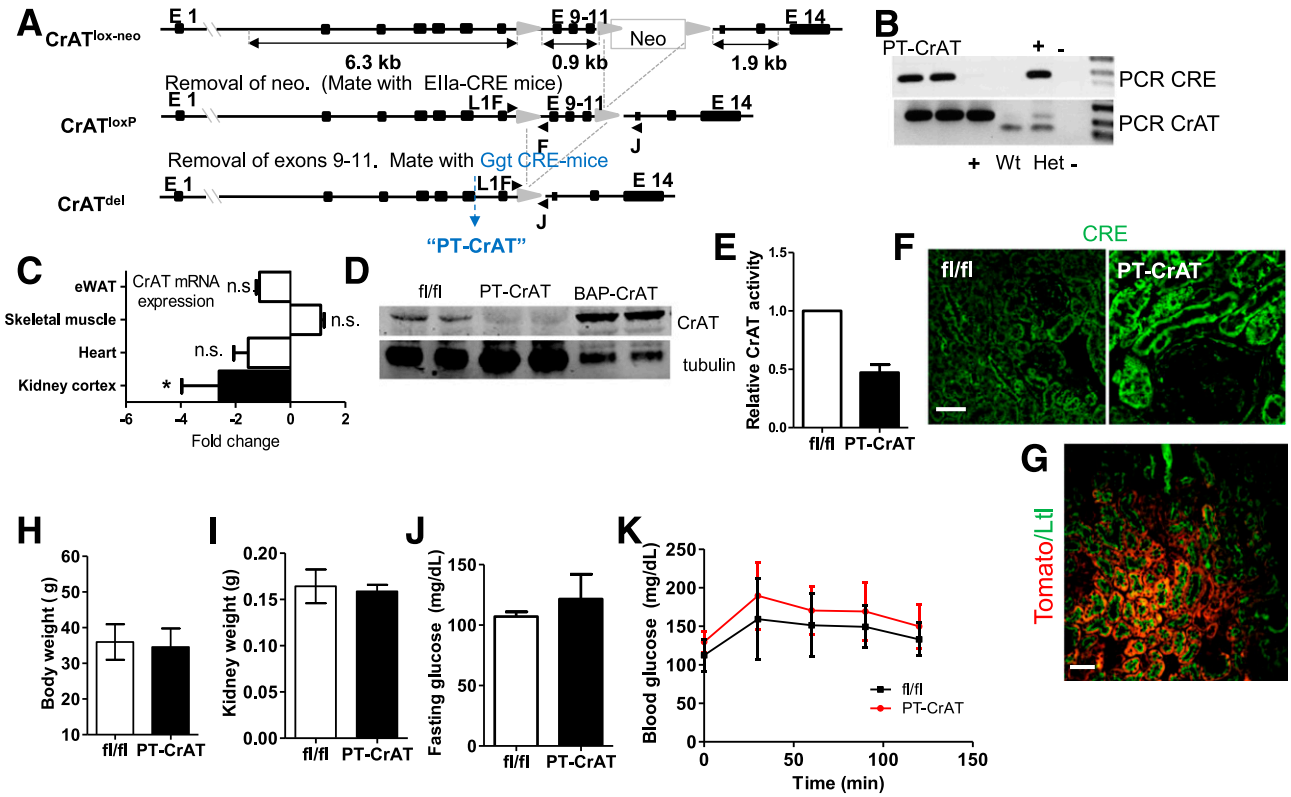

Figure 1—Generation of PTC-specific CrAT knockout mouse and baseline whole-body parameters. *A*: Genetic strategy to generate mice with PTC-specific ablation of CrAT (PT-CrAT mouse). *B*: Deletion was confirmed by PCR in tail DNA. *C*: CrAT knockout kidney cortices, but not heart, skeletal muscle, or epididymal white adipose tissue (eWAT), showed a ~2.6-fold reduced expression of CrAT mRNA ($n = 6$). *$P <$ 0.006, *Gapdh* reference gene. *D*: Western blot analysis of CrAT protein levels in kidney cortices showed successful deletion in the PT-CrAT mice. Kidney and skeletal muscle tissues from mice overexpressing CrAT under the β-actin promoter (BAP-CrAT) were used as positive control. *E*: Enzyme activity was measured in whole-kidney homogenates (residual CrAT activity derives from cells other than PTCs). PTC-specificity was verified by staining for CRE activity with an anti-Cre antibody (*F*) and by breeding PT-CrAT female mice with a *tdTomato* male (*G*). Red fluorescence around green brush borders stained positive by *Lotus tetragonolobus* lectin confirms PTC-specific Cre activity. Scale bars = 50 μm. PT-CrAT mice body weights (*H*), kidney weights (*I*), fasting blood glucose levels (*J*), and glucose tolerance test (*K*) (males, $n = 6$–8).

Immunostaining

Deparaffinized kidney sections were mounted on Superfrost slides, permeabilized with 0.1% Triton-X, and blocked with 1% BSA. Antibodies were diluted in PBS and applied on kidney sections using a PAP Pen to create a hydrophobic barrier: rabbit anti-collagen IV, 1:250 (Abcam); mouse anti-vimentin, 1:250 (Sigma-Aldrich); cleaved caspase-3, 1:200 (Abcam); *Lotus tetragonolobus* anti-lectin conjugated with green fluorophore (488 nm), 1:200 (Vector Laboratories); and corresponding Alexa Fluor 598 red anti-mouse or Alexa Fluor 647 cyan anti-rabbit secondary antibodies, 1:750 (Thermo Fisher). Slides were coverslipped (Fluoromount-G) and observed using a Leica DM6000 fluorescent microscope.

Western Blotting

Kidney cortices were homogenized in lysis buffer and normalized for protein concentration. Proteins were separated using gel electrophoresis, transferred onto a nitrocellulose membrane, and analyzed by standard Western blotting methods using the following antibodies: rabbit anti-CrAT, 1:250 (Proteintech); mouse anti–4-hydroxynonenal (4-HNE), 1:500 (R&D Systems); mouse anti–acetyllysine, 1:500 (Cytoskeleton); mouse anti-OxPhos cocktail, 1:500 (Thermo Fisher); and mouse anti–β-actin or tubulin as loading control when applicable, 1:5,000. Secondary antibodies (anti-mouse or anti-rabbit, 1:5,000; conjugated with horseradish peroxidase) (Thermo Fisher) were applied at room temperature for 1 h. Band intensities were measured using the ImageJ software Gel Analysis plug-in.

Primary Cell Culture and Mitochondrial Respiration Analysis

Kidneys from younger PT-CrAT and fl/fl mice (<9 months) were harvested and placed into ice-cold Krebs-Henseleit buffer for primary proximal tubular epithelial cell isolation. PTCs were isolated using a collagenase digestion/sieve/Percoll gradient centrifugation method originally described by Vinay et al. (28). Cells were grown in hormonally defined DMEM media (28). Once cells reached near confluency (~day 7–8), they were plated onto 24-well Seahorse XF24 culture plates (75,000 cells/well). Mitochondrial oxygen

consumption was measured in cells respirating on 5 mmol/L pyruvate using a Seahorse XF24 Extracellular Flux Analyzer.

Mitochondrial Complex Activities

Complex I and complex V activity was measured from repeatedly freeze-thawed kidney cortex homogenates by following the oxidation of NADH at 340 nm. For complex I activity, the final reaction mixture contained 62.5 μmol/L ubiquinone, 0.25% BSA, 2 μg/mL antimycin A in 25 mmol/L potassium phosphate buffer (pH = 7.2), and the sample equivalent to 10 μg protein. Oxidation of NADH was followed at 340 nm in the absence and presence of 10 μg/mL rotenone (3 min each). For complex V activity, the mixture contained the sample equivalent to 5 μg protein, 10 μL of 30 mmol/L NADH, 50 μL of 50 mmol/L phosphoenolpyruvic acid, 5 μL of 10 mg/mL pyruvate kinase, 10 μL of 5 mg/mL lactate dehydrogenase, and 10 μL antimycin A in 900 μL HEPES-Mg^{2+} buffer (pH = 8.0) at 30°C. Baseline was recorded for 2 min, then 100 μL of 25 mmol/L ATP was added and the absorbance recorded for another 2 min. Then 10 μL of 0.2 mg/mL oligomycin was added and the absorbance was recorded again for 2 min. In both cases, V_{max} values were calculated from the kinetic graphs, and activities were expressed as control percentage.

Mass Spectrometry

Kidney cortex, plasma, and urinary levels of acylcarnitines and organic acids were measured using flow injection tandem mass spectrometry (MS/MS) at the Duke-National University of Singapore (29,30).

Electron Paramagnetic Resonance Spectroscopy

A cohort of mice received the spin trap POBN (α-[4-pyridyl *N*-oxide]-*N*-*tert*-butylnitrone) (500 mg/kg i.p.) 45 min before euthanasia to analyze lipid-derived free radical production. Kidney samples were extracted using a Folch extraction method (31,32). Extracts were analyzed in a quartz flat cell using an X-band EMXplus EPR Spectroscope (parameters: 3,480 ± 80 G scan width, 10^5 receiver gain, and 20 mW microwave power; time constant: 1,310 ms; conversion time: 655 ms).

Quantitative PCR

Total RNA from kidney cortices was used for real-time quantitative (q)PCR to compare gene expressions (*Vim*, *Col4A1*, *Col3A1a*, *Fn*, *Bax*, and *Casp-3*) between groups using SYBR Green Master Mix as described by the manufacturer (Applied Biosystems). Fold changes in gene expression were calculated using the ΔΔCT method.

Albumin and Creatinine

Urinary albumin levels from 24-h urine samples were measured using the Albuwell M albumin kit (Exocell). Creatinine levels in serum and urine were measured using the Creatinine Companion kit (Exocell). Albuminuria was expressed as albumin-to-creatinine ratios (μg/mg) according to the Animal Models of Diabetic Complications Consortium recommendation.

Statistical Analysis

Data are expressed as mean ± SD. Statistical significances between fl/fl and PT-CrAT mice or PT-CrAT mice on LFD versus PT-CrAT mice fed the HFD were determined by unpaired Student *t* test.

RESULTS

PT-CrAT Mice Develop Tubular Disease and Secondary Glomerulosclerosis

Mice with PTC-specific deletion of CrAT were created using a Cre-loxP strategy, genotyped, and characterized as detailed in Fig. 1. CrAT deletion was specific to the proximal tubules (Fig. 1*B*–*G*). The first cohorts of mice were fed the chow diet, and for consistent development of nephropathy (33), were aged to >12 months. Renal tissue was examined every 3 months. PT-CrAT mice had normal body weights (Fig. 1*H*), kidney weights (Fig. 1*I*), fasting blood glucose levels (Fig. 1*J*), and glucose tolerance (Fig. 1*K*). They developed tubular disease with protein casts, tubular dilation, and fibrosis at ~18–20 months of age (Fig. 2*B* and *C*). Increased levels of collagen IV, vimentin, and cleaved caspase-3 were detected in PT-CrAT mice using immunofluorescent techniques (Fig. 2*F*–*I*). By this time, they also had increased serum creatinine levels and proteinuria (Fig. 2*D* and *E*). Consistently with the stainings, significantly increased expression levels of vimentin, collagen IV, Bax, and caspase-3 were detected by qPCR, indicating fibrosis and activation of apoptosis regulators (Fig. 2*J*). Interestingly and unexpectedly, PT-CrAT mice also developed glomerulosclerosis. Within a given cohort of mice, tubular/glomerular disease and proteinuria always varied to an extent, with some mice having only mild changes and others having extensive damage. These results indicate that ablation of CrAT in the PTC leads not only to tubular disease but also to proteinuric CKD and facilitates tubular cell/mitochondrial apoptosis.

PT-CrAT Mice Have Altered Acylcarnitine and Organic Acid Profiles

Next, to determine the extent of mitochondrial overload, we measured the levels of acylcarnitine products in fl/fl and PT-CrAT mice plasma, kidney cortex, and urine. Figure 3*A*–*C* shows the results of a detailed MS/MS analysis of major acylcarnitine species. PT-CrAT mice displayed altered acylcarnitine profiles in the kidney cortex and urine compared with fl/fl littermates. Notably, CrAT deficiency in the PTC led to a significant decrease in the levels of acetyl and several other short- and medium-chain acylcarnitines. This result is consistent with the hypothesis of mitochondrial overload: because of the lack of CrAT in PTCs, efflux capacity is attenuated, and thus, short-chain acylcarnitine levels are much lower in the cortex and urine. Interestingly, and also consistent with previous observations in skeletal muscle (23), many of the

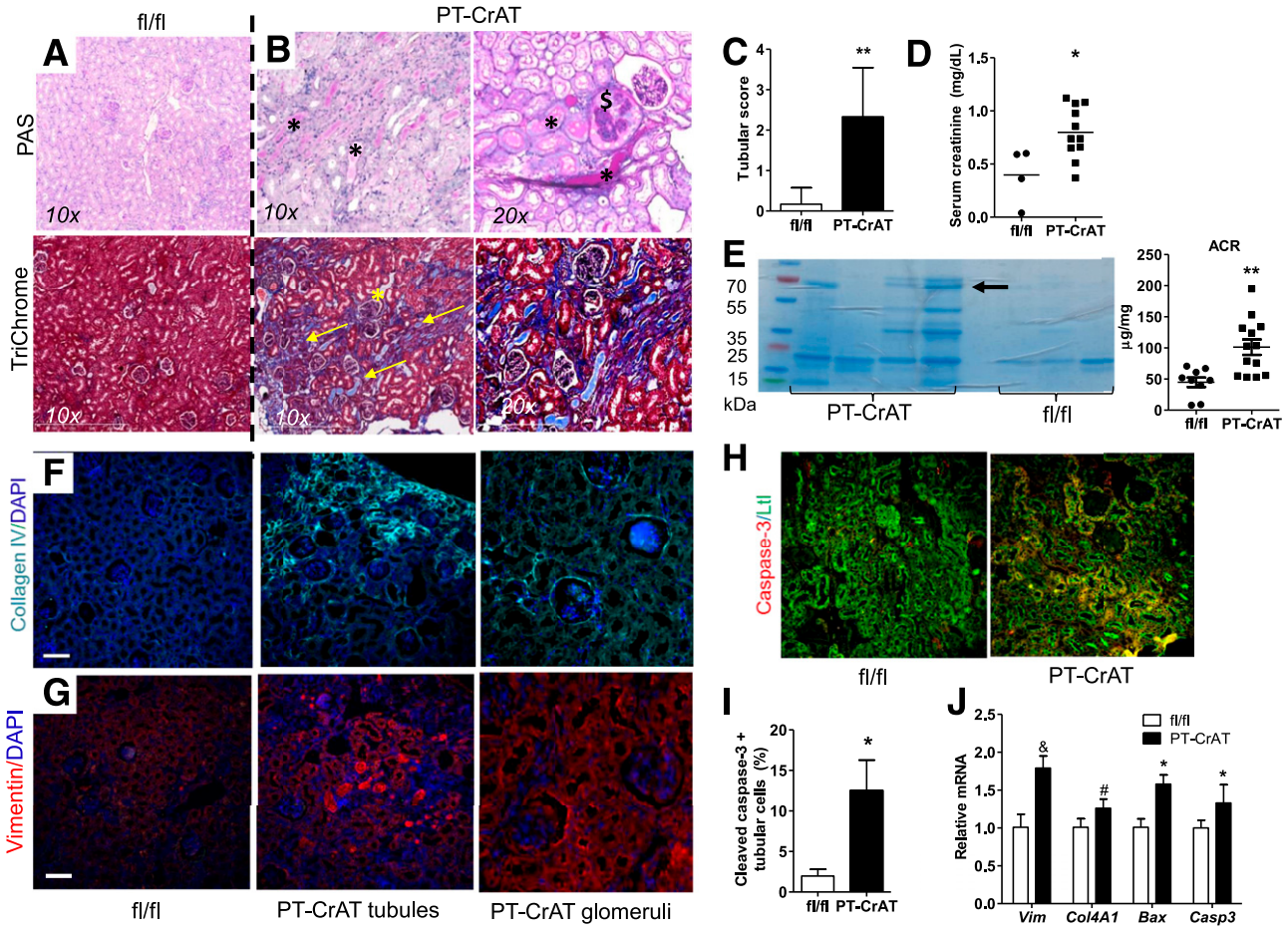

Figure 2—CrAT deletion in PTCs causes kidney disease. *A*: Representative photomicrographs of PAS and trichrome staining in fixed, paraffin-embedded fl/fl kidneys showing normal histology. *B*: PT-CrAT kidneys show numerous protein casts in tubular lumen, tubular dilation (*), lipid droplets in tubular cells, trichrome-positive material/fibrosis (yellow arrows), and secondary glomerular disease ($) (≥18 months). *C*: Tubular injury area was evaluated semiquantitatively, and scores are expressed as minimal 1: <5% of cortex, mild 2: 5–24%, moderate 3: 25–49%, and severe 4: >50% of cortex ($n = 6$). $^{**}P < 0.005$. *D*: Serum creatinine levels in fl/fl and PT-CrAT mice ($n = 4$–10). $^{*}P < 0.05$. *E*: Urine protein analysis by electrophoresis/Coomassie blue staining (arrow points at albumin, ~67 kDa) in PT-CrAT mice compared with fl/fl controls, with equal amounts of protein (20 µg) loaded and urinary albumin-to-creatinine ratios (ACR) (males, $n = 8$–12). $^{**}P < 0.005$. Staining positive for collagen IV (cyan: collagen IV, blue: DAPI) (*F*) and vimentin (red: vimentin, blue: DAPI) (*G*) in PT-CrAT tubules and glomeruli. (Photomicrographs are from mice with the highest tubular injury scores.) *H*: Active caspase-3 staining (red: cleaved caspase-3, green: *Lotus tetragonolobus*) in fl/fl and PT-CrAT kidneys. Scale bars = 50 µm. *I*: Percentage of apoptotic PTCs was evaluated by counting cleaved caspase-3–positive, *Lotus tetragonolobus* counterstained cells ($n = 4$). $^{*}P < 0.05$. *J*: Gene expression analysis in fl/fl and PT-CrAT kidney cortices ($n = 6$, male mice). $^{*}P < 0.05$, #$P < 0.01$, &$P < 0.0005$ vs. fl/fl.

longer-chain acylcarnitine levels were increased in the kidney cortex. Furthermore, several of the measured organic acid levels (citrate, fumarate, malate, lactate, and pyruvate) were depleted in the PT-CrAT cortex (Fig. 3*G*). We also found an approximately twofold increase in urinary levels of free and total carnitine in the PT-CrAT mice, although these differences did not reach statistical significance (Fig. 3*D*–*F*). Carnitine loss to the urine suggests that secondary carnitine insufficiency could develop that may be attributable to PTC injury (34).

Lipid-Derived Free Radical Production Is Increased in PT-CrAT Mice

Retaining incompletely oxidized acylcarnitine products in the mitochondria can lead to conditions favorable for redox imbalance. This is because mitochondrial overload may produce reducing equivalents (NADH and $FADH_2$) in excess of that which can be handled by the ETC (22,25). Such excess in turn is predicted to create an environment conducive to oxidative stress. Excess ROS in a membrane-rich environment, such as the mitochondrial inner membrane, then would increase the odds for lipid peroxidation (35–37). To address this scenario, we used electron spin resonance spectroscopy and in vivo spin trapping to measure the levels of lipid-derived free radicals in kidney cortices. Results were also confirmed by Western blot analysis of 4-HNE adducts. Figure 4*A* shows spectra obtained from fl/fl and PT-CrAT mouse kidney cortex extracts. PT-CrAT kidney cortices display an approximately threefold increase in carbon-centered lipid-derived

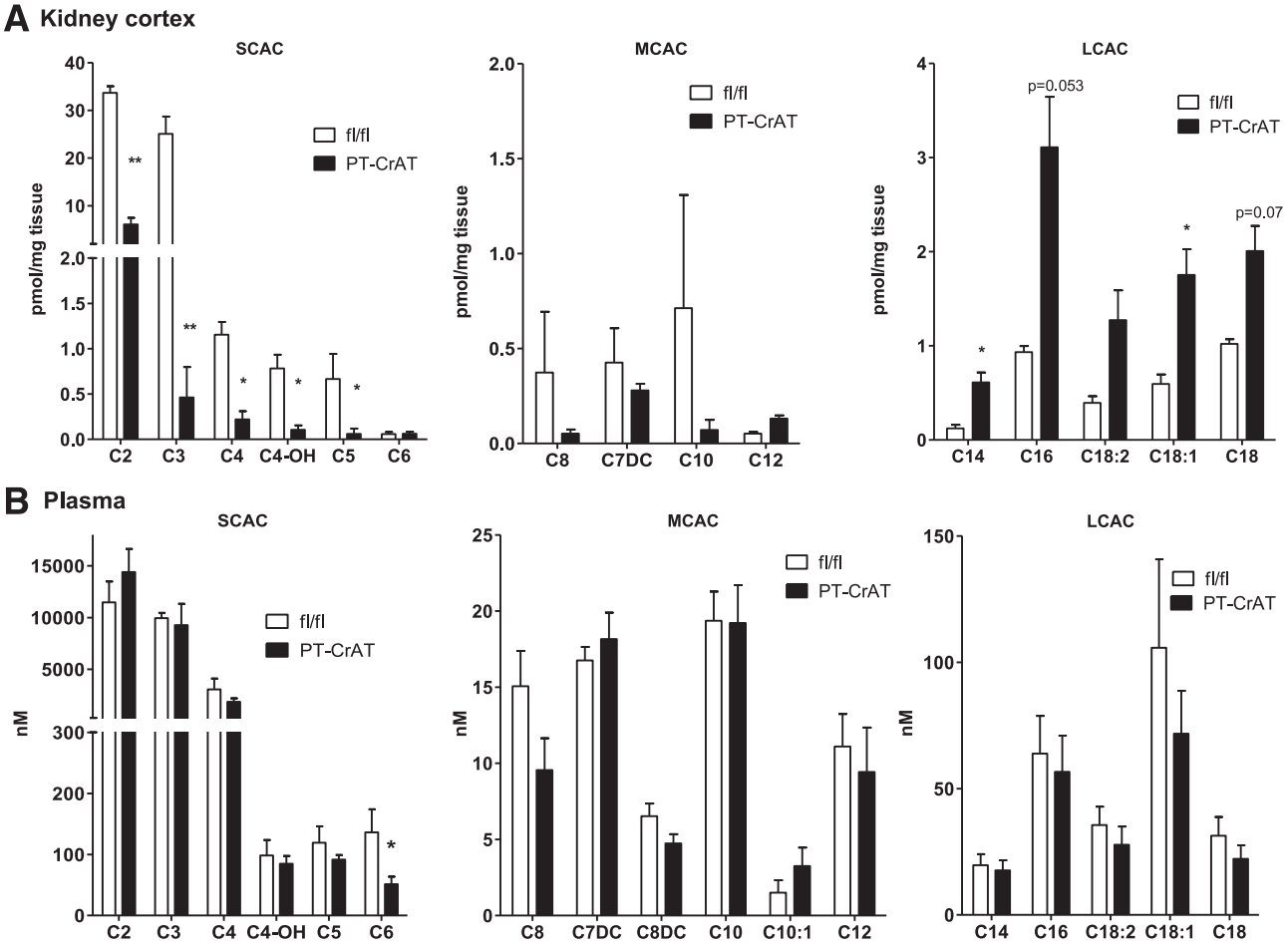

Figure 3—Altered acylcarnitine and organic acid profiles in the PT-CrAT model. Kidney cortex (*A*), plasma (*B*), and urine samples (*C*) from PT-CrAT mice and fl/fl controls at 18–24 months of age were analyzed by MS/MS for short- (SCAC), medium- (MCAC), and long-chain acylcarnitines (LCAC), as well as free (*D*) and total carnitine levels (*E*). MS/MS analysis was normalized to show mice with the strongest kidney injury histology scores. *F*: Free-to-total carnitine ratios indicating urinary wasting of free carnitine are shown. *G*: Kidney cortices were analyzed for organic acid intermediates. α-ketogl., α-ketoglutarate. **P* < 0.05, ***P* < 0.005 vs. fl/fl.

free radical production compared with fl/fl littermates. We consistently found a significant increase of 4-HNE adducts in CrAT-ablated cortices (Fig. 4*B* and *C*). These results confirm that mitochondrial overload may increase ROS production, which then also triggers excess lipid peroxidation.

HFD Challenge Accelerates Kidney Disease in PT-CrAT Mice

Next, we asked whether obesity and prediabetes-induced renal injury are accelerated by mitochondrial overload. We used the HFD challenge to determine whether PT-CrAT mice are more susceptible to HFD-induced renal disease. HFD feeding led to an earlier manifestation (12–15 months) of CKD in the PT-CrAT model (Fig. 5*A*–*C*). Compared with fl/fl littermates fed the HFD or with PT-CrAT mice fed the LFD, PT-CrAT mice fed the HFD had larger glomeruli (Fig. 5*D*) and increased expression of fibrosis genes *Vim, Fn*, and *Col3A1a* (Fig. 5*E*). Systemic changes, such as body weights, plasma triglyceride, and free fatty acid levels, however, were comparable between PT-CrAT colonies, regardless of the diet (Fig. 5*F*–*H*). Thus, CrAT deletion in the PTC promotes obesity/prediabetes-related kidney disease and, potentially through secondary mechanisms, affects glomerular structure.

Primary PTCs From PT-CrAT Mice Have Energy Deficit and Impaired Mitochondrial Respiration

To further assess mechanistic details related to mitochondrial overload, we isolated primary PTCs from fl/fl and PT-CrAT mice. PTCs were isolated from younger mice (up to 9 months) where pathology was not yet present. When mitochondrial oxygen consumption rates were compared in an XF24 Analyzer, cells from the PT-CrAT mice displayed significantly lower basal, ATP-linked, and maximal respiration (Fig. 6*A* and *B*). These results indicate early changes in mitochondrial respiratory function and energy deficit (lower ATP-linked respiration) in PTCs with mitochondrial overload. Importantly, because these alterations

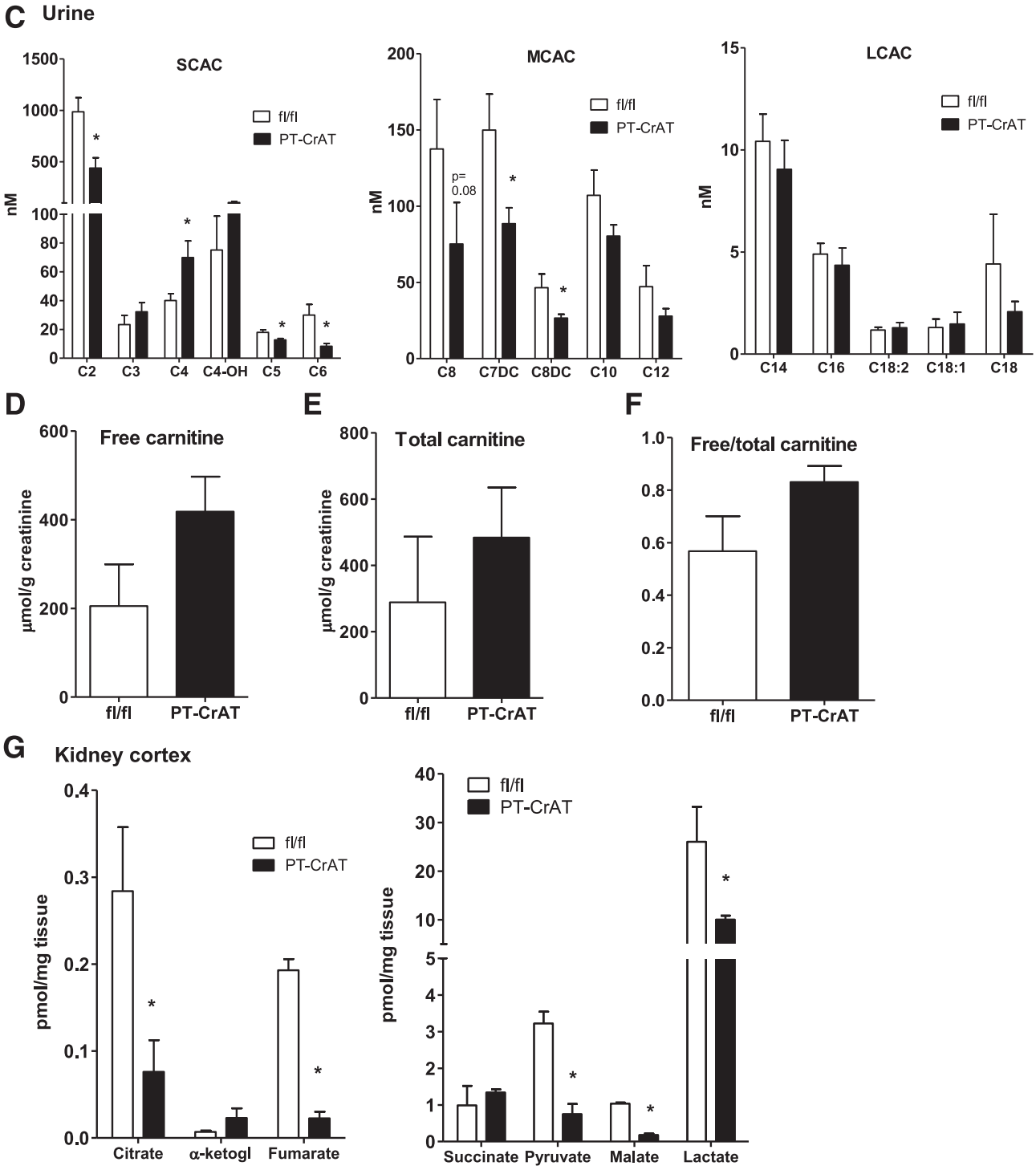

Figure 3—*Continued.*

are present before pathology develops in the PT-CrAT mice, mitochondrial dysfunction and energy deficit could be a primary cause of tubular cell death later. Tissue abundance of mitochondrial ETC complexes or the amount of total acetyl-lysine modified proteins were not different between groups (Fig. 6*C* and *D*), indicating similar mitochondrial content in control and CrAT-ablated mice. However, complex I and complex V activities were impaired (Fig. 6*E*).

DISCUSSION

Mitochondrial overload was first described in skeletal muscle in relation to the development of insulin resistance (22,25). The effects of CrAT deletion were also demonstrated first

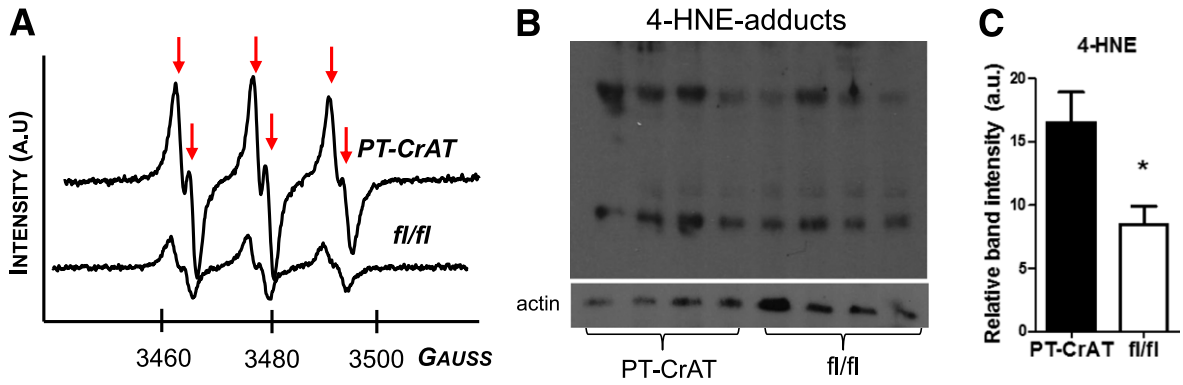

Figure 4—PT-CrAT mice have increased lipid-derived free radical levels. *A*: Representative spectra of POBN-lipid radical adducts detected by electron spin resonance spectroscopy from Folch extracts of kidney cortex of PT-CrAT mice and fl/fl littermates ($n = 5$). Increases in the amplitude of the six line spectrum peaks (arrows) are proportional to an increase in carbon-centered lipid-derived free radical levels. Spectra show an approximately threefold increase of lipid radicals in the PT-CrAT mice vs. fl/fl control. a.u., arbitrary units. *B*: Western blot analysis detected 4-HNE protein adducts. *C*: Band intensities (normalized to β-actin as loading control) were measured using ImageJ ($n = 4$). *$P < 0.05$ vs. fl/fl.

in skeletal muscle, with many of the results resembling a scenario that models one specific aspect of obesity or metabolic disease: overabundance of substrates to the mitochondria (23). In relation to DN and CKD, there is limited information available on carbon trafficking, substrate overabundance, and the effects of dysfunction of mitochondrial enzymes regulating such functions in the kidney. PTCs rely heavily on mitochondrial fatty acid oxidation for their energy needs (6), but how deviations in fatty acid oxidation affect the tubules is not entirely clear.

Our previous work in cell culture showed that mitochondrial entry of fatty acids is required for PTC apoptosis rather than just cytoplasmic lipid accumulation (38). Here, we provide evidence that when cellular/mitochondrial acyl-CoA balance and thus mitochondrial carbon trafficking is disturbed, mice develop kidney disease. Pathological features included tubular dilation, proteinaceous casts, fibrosis, proteinuria, and, interestingly, enlarged glomeruli and copious amounts of glomerular scarring. Importantly, these changes can be attributed to the tubular deletion of CrAT and are likely not caused by other whole-body metabolic alterations because mice display normal body weight and fasting glucose and respond normally on the glucose tolerance test. Thus, our results indicate that a specific metabolic defect, driven by the deletion of a single gene of an important metabolic enzyme in PTC mitochondria, is sufficient to cause tubular disease. PT-CrAT mice recapitulate many features of metabolic disease–related nephropathies, but without the confounding factors deriving from changes in whole-body metabolism during diabetes. Therefore, it is a useful model to exclusively study the effects of mitochondrial derailments and substrate overload, without a number of additional factors that would derive from a diabetes model. Notably, PT-CrAT mice presented some range in the severity of pathology. This cannot fully be attributed to the genetic background because mice were created on the C57BL/6 background, and the original Ggt-Cre mice (mixed Balb/cJ/C57BL background) were crossed into the C57BL/6 background for generations during the development and breeding of the cohorts. It is, however, consistent with previous findings from other mouse models of renal disease or human nephropathies where varying degrees of phenotypic changes are a characteristic feature (39–42).

Our results are in good agreement with those obtained by skeletal muscle–specific *crat* deletion. Many of the short-chain acylcarnitines were present in significantly lower concentrations in the cortex and urine, with a concomitant increase of several of the medium- to long-chain acylcarnitines. The reduction in the levels of the short-chain acylcarnitines was more striking than initially expected. These results suggest that CrAT in the PTC is absolutely essential to maintain the levels of these metabolites. Reduction in the levels of some of the odd-chain metabolites (C3 and C5, in particular) reveals a more global effect on substrate metabolism, because these acylcarnitines are derived primarily from branched-chain amino acid metabolism. Plasma levels of most of the acylcarnitines examined were not altered significantly, indicating that other tissues (such as skeletal muscle) are more likely significant contributors of circulating acylcarnitine levels.

In healthy individuals, carnitine esters are excreted into the urine. Impairments in acylcarnitine excretion occur with deteriorating renal function (43). Thus, our findings of altered acylcarnitine profiles in the PT-CrAT mice may also suggest slowly declining renal function when PTC mitochondrial carbon trafficking is disturbed. There is also resemblance to a type 2 diabetic muscle. In patients with type 2 diabetes, CrAT mRNA abundance is ∼80% lower in skeletal muscle compared with healthy individuals (23). In diabetic rats, accumulation of long-chain acylcarnitines was accompanied by lower free carnitine levels

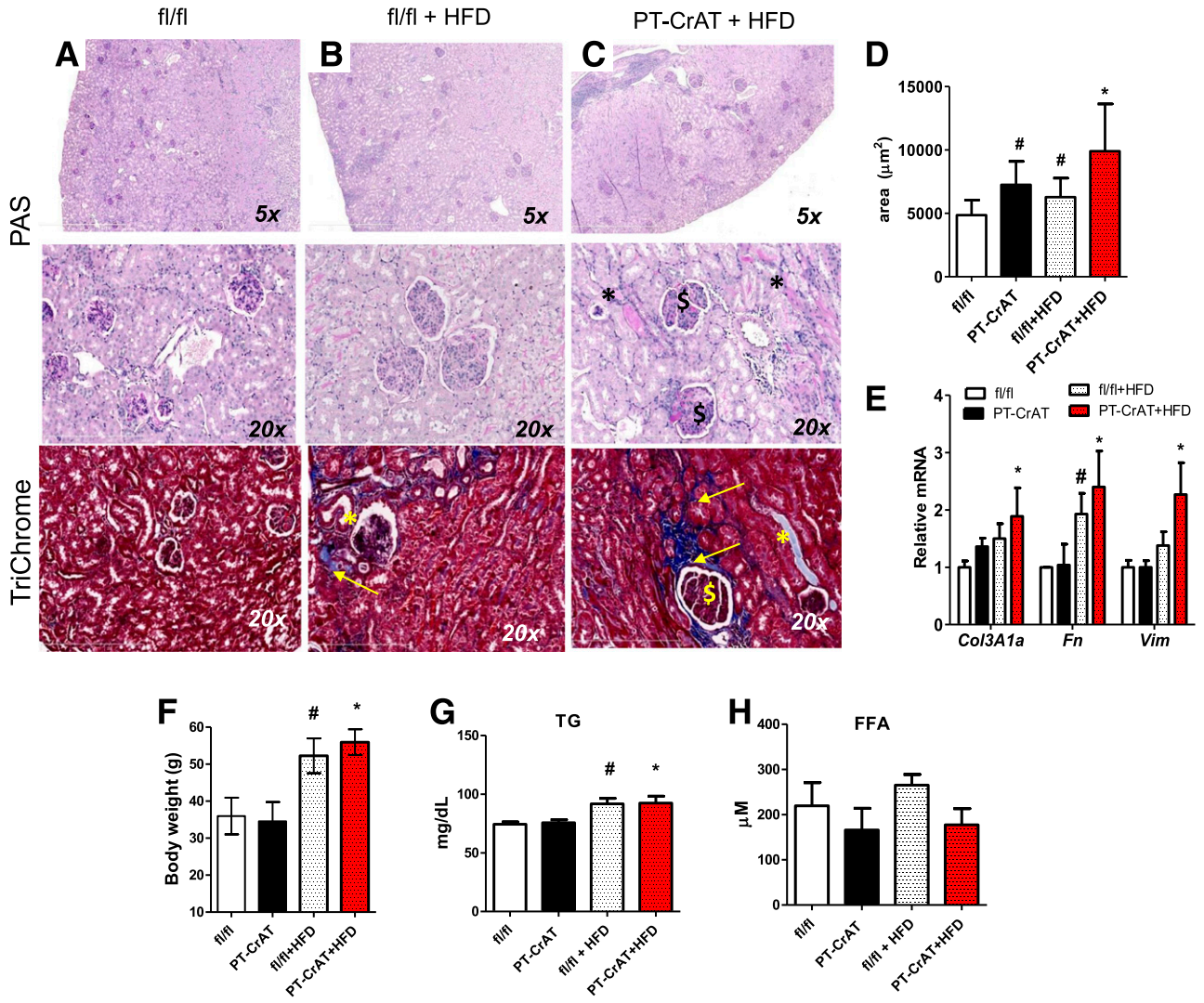

Figure 5—The HFD accelerated kidney disease in the PT-CrAT mice. Representative photomicrographs of PAS- and trichrome-stained kidneys of littermate fl/fl mice showing normal histology (*A*), fl/fl mice fed the HFD (*B*), and PT-CrAT mice fed the HFD (*C*) showing tubular damage (*), fibrosis, and trichrome-positive material (yellow arrows), as well as glomerular sclerosis ($) and glomerulomegalia (12–15 months). *D*: Glomerular tuft size was measured in each group (n = 30–50 glomeruli per group, at 12 months of age). Gene expression analysis in kidney cortices (*E*), body weights (*F*), plasma triglyceride (*G*), and free fatty acid levels (*H*) in each experimental group (n = 4–6). #$P < 0.05$ vs. fl/fl on chow diet, *$P < 0.05$ vs. PT-CrAT on chow diet.

(44). Carnitine loss to the urine in our model thus suggests that there may be lower free carnitine levels in the kidney or that there is carnitine loss due to an increase in injured PTCs in the PT-CrAT mice. Accumulation of long-chain intermediates was coupled with depletion of several of the organic (TCA) intermediates. This observation is consistent with earlier ones in different organs where heightened β-oxidation appeared to reduce the levels of TCA intermediates (22). Such results may reflect compromised mitochondrial status. Markedly reduced pyruvate and lactate levels also suggest impairments in carbohydrate metabolism.

Susztak and colleagues (10) studied derailments in fatty acid oxidation, focusing on the mitochondrial fatty acid import side. Their studies demonstrated lower expression of carnitine palmitoyltransferase (Cpt1a) in kidneys from DN patients or in mice with tubulointerstitial fibrosis. Cpt1 facilitates the import of long-chain fatty acyl-CoAs into the mitochondria for β-oxidation (45,46). Defects in fatty acid oxidation caused by downregulation or inactivity of Cpt1 are detrimental to the tubules. In light of the data of the Susztak group and ours, it seems that not only defective mitochondrial fatty acid oxidation but also a failure to remove excess acetyl-CoA and acylcarnitine products promotes kidney disease. Because acetyl-CoA is a central metabolic intermediate, acetyl-CoA–to–CoA imbalance in the PTC appears to affect all three major nutrient metabolism pathways. Because the glycolytic ability of the PTC is not significant and thus "substrate switching"—unlike in skeletal muscle—is not prominent

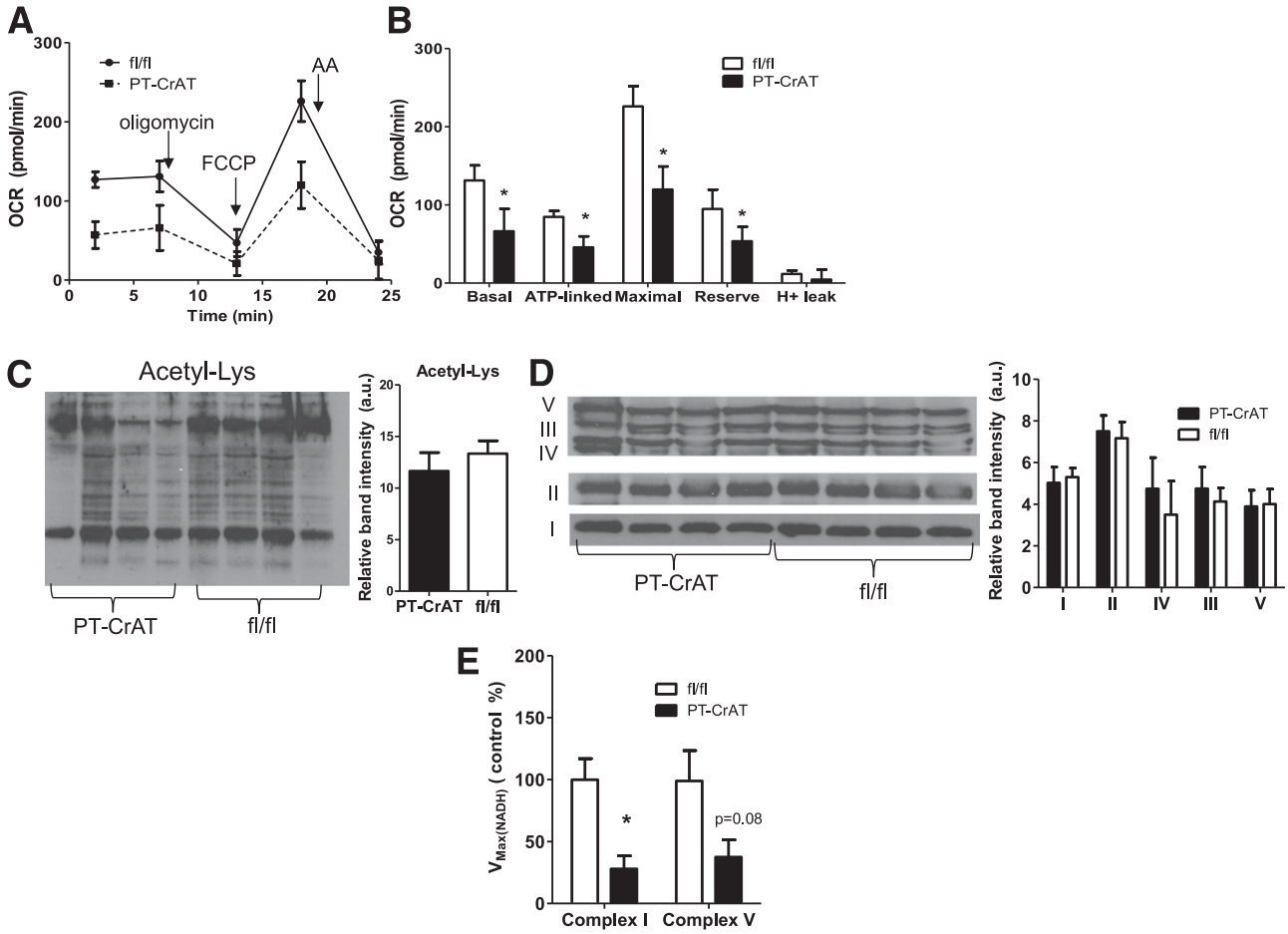

Figure 6— Primary PTCs from PT-CrAT mice have early alterations in mitochondrial respiratory function. PTCs isolated from fl/fl and PT-CrAT mouse kidneys (9 months) were grown on Seahorse XF24 plates (75,000 cells/well). *A*: Mitochondrial oxygen consumption rates (OCR) were measured at baseline and after the addition of 2 μmol/L oligomycin, 2 μmol/L FCCP, or 1.5 mg/mL antimycin A (AA). *B*: Mitochondrial respiratory parameters were calculated and compared from the graph shown on *A* (n = 10). *$P < 0.05$ vs. fl/fl. Total acetylated lysine (Acetyl-Lys) levels (*C*), abundance of mitochondrial ETC complexes (*D*), and activity of mitochondrial complex I and V in kidney cortices of fl/fl and PT-CrAT mice (n = 4) (*E*). a.u., arbitrary units. *$P < 0.05$ vs. fl/fl.

in the tubules, we propose that PTCs can handle an abundance of lipid-based substrates as long as the mitochondrial influx or efflux capacity of substrates/products is not compromised. Cpt1 and CrAT deficiencies both seem to accompany the development of type 2 diabetes and could therefore be significant contributors to tubular damage in CKD/DN.

Regarding ROS production, a prevailing theory is that acetyl-CoA is the main fuel for the TCA cycle but that an overabundance of acetyl-CoA will produce reducing equivalents (NADH and $FADH_2$) in excess of what can be handled by the ETC (22,25). This excess in turn creates an environment conducive to oxidative stress through the "backflow" of electrons from complex III toward complex I (25,47). Such redox pressure may exist regardless of whether TCA activity is increased (early diabetic kidney disease) or decreased (late diabetic kidney disease) (19) because heightened β-oxidation will provide excess NADH and $FADH_2$. The "backflow" can change the reduced/oxidized state of the ETC complexes, leading to slower or diminished ATP production as a potential mechanism contributing to PTCs' energy deficit. Our data confirm that CrAT ablation increases the steady-state levels of lipid peroxide radicals as well as their end products, 4-HNE, in kidney cortex. Our results also suggest that in a lipid-rich environment such as the mitochondria, with ROS production sites close to membrane structures, the odds are increased for lipid radical production and lipid peroxidation.

This may not, however, be the only mechanism contributing to cell damage or may only be limited to the mitochondria. Excess acetyl-CoA can also drive acetylation of proteins, particularly the proteins of the ETC. In this regard, lysine acetylation of mitochondrial proteins has been gaining attention as a prominent posttranslational modification causing cellular stress, where the buffering capacity of CrAT was highlighted (47). Modification of ETC proteins could then cause a slowdown in ATP production. Although there were no detectable differences in the levels of Lys acetylated proteins between control and

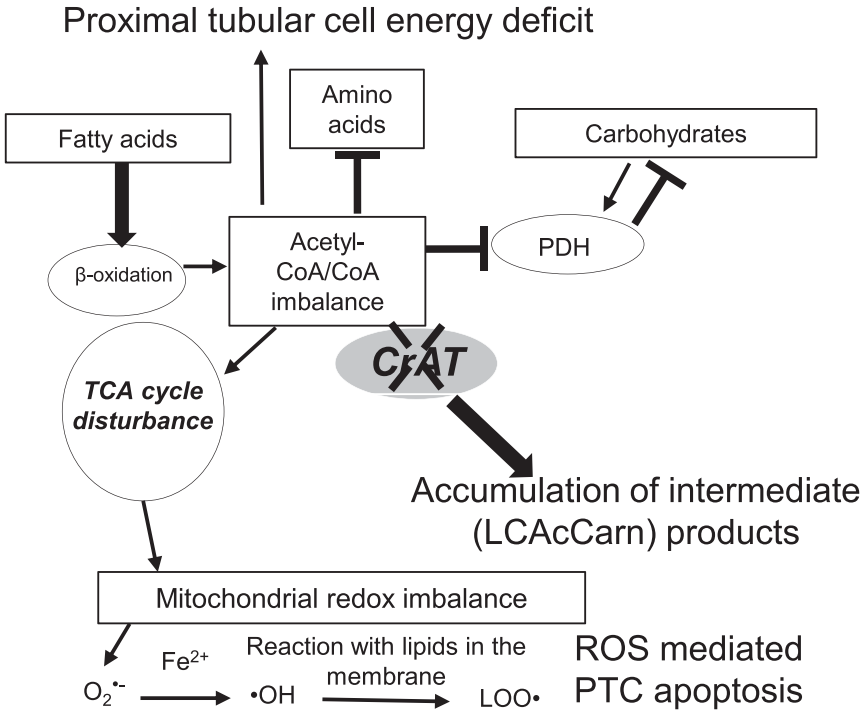

Figure 7—A proposed scenario of mitochondrial overload in PTCs. Mitochondrial overload modeled by CrAT deletion causes acetyl-CoA/free CoA imbalance and leads to the accumulation of incompletely oxidized products. Such imbalance affects all three major metabolic pathways in PTCs: fatty acid, amino acid, and carbohydrate metabolism. As shown by our mass spectrometry results, overload also affects TCA cycle metabolite levels. Altogether, these metabolic disturbances can contribute to PTC energy deficit. Furthermore, overload can cause mitochondrial redox imbalance through affecting the ETC. Increased ROS and lipid peroxide production then also potentially contributes to PTC apoptosis.

CrAT-ablated mice in kidney cortex homogenates (Fig. 6*C*), acetylation as a posttranslational modification is still worthy of further investigation. Detailed analysis in isolated mitochondria or challenging permeabilized mitochondria with acetyl-CoA + carnitine addition may reveal differences in how mitochondrial overload can trigger such modifications.

Our data also reveal mitochondrial energy deficit and respiratory impairments as a potential mechanism leading to tubular injury, because these alterations are present before the onset of significant pathology. Primary PTCs isolated from the PT-CrAT mice at ~9 months of age grew well in hormonally defined DMEM. At the same cell density, however, their mitochondrial respiration was significantly lower than those isolated from littermate fl/fl mice (Fig. 6). Most importantly, PTCs from PT-CrAT mice displayed energy deficit and lower ATP-linked respiration, suggesting that indeed, tubular mitochondrial acetyl-CoA imbalance leads to derailments in mitochondrial energy production. If PTC mitochondria are not able to meet the energy need of tubular cells, this could lead to significant deficits in, for example, tubular epithelial function such as Na^+/K^+ ATPase activity. It is noteworthy that we only tested these primary cells respirating on pyruvate; therefore, we cannot conclude whether PTCs lacking CrAT would respirate differently on other substrates such as, for example, succinate or glutamate/malate. As it has been proposed before that excess acetyl-CoA is able to block PDH activity (23), a possible interpretation of our result is that PTCs with CrAT ablation cannot efficiently catabolize pyruvate. Mitochondrial content and abundance of ETC complexes was not different between normal and CrAT-ablated mice; however, activities of complex I and complex V were reduced. It is therefore likely that functionality or oxidized/reduced state of such complexes and/or one or more of their subunits are altered. Further investigation into mitochondrial structure, pathways, and function is warranted, which was ongoing in our laboratory at the time this report was finalized. This includes electron microscopy analysis of mitochondrial structure, functional analysis of PT-CrAT tubular cells, and a detailed next-generation sequencing analysis of PT-CrAT cortices along a full timeline from 3 to 24 months to understand causality.

Our findings about secondary glomerulosclerosis are puzzling. Because CrAT has only been deleted in the proximal tubules, we suspect this is an indirect effect resulting from initial tubular damage. Also noteworthy is that regardless of the variability of the phenotype (mild to more severe in the PTC), we consistently found secondary sclerosis in all of our cohorts. Similar findings have been reported before. Bonventre and colleagues (48) found

that repeated, selective tubular epithelial injury led to secondary glomerulosclerosis. The authors surmised that this effect could be attributed to a paracrine signaling mechanism derived from injured/regenerating epithelium or to a reduction of glomerular blood flow as a result of decreased loss of capillaries in tubulointerstitial fibrosis. It is also possible that a progressive tubulointerstitial reaction may directly encroach upon the glomerular tuft, causing the narrowing and disconnection of the glomerulotubular junction (49–51). These results warrant further studies to determine the exact cause of glomerulosclerosis observed in the PT-CrAT model.

CrAT deletion also further sensitized mice to HFD-induced renal injury. We surmise that this is because excess substrate caused by the chronic lipid exposure further compromises mitochondrial acetylcarnitine and short-chain acylcarnitine efflux capacity. These metabolites, together with a further surplus of reducing equivalents, may block several metabolic enzymes (through allosteric inhibition) and mitochondrial ETC proteins. The result is an exacerbated overload affecting the kidney.

Taken together, PTC-specific ablation of CrAT causes tubular injury, glomerulosclerosis, and kidney disease in mice. We believe our results are in agreement with those supporting the view that proximal tubular damage is also a primary rather than just a secondary event in early DN. The results are consistent with mitochondrial overload, showing chronic effects in vivo: impaired nutrient utilization, which is not limited to fatty acid oxidation (Fig. 7). These results provide the basis for future studies to decipher the acute effects and a potential protection from overload. This can be achieved, for example, through overexpressing CrAT in cultured tubular cells and then challenging these cells to overload. In vivo, however, such an approach might not provide additional protection in case of an abundant metabolic enzyme like CrAT. Our in vivo results point to a much broader approach to tackle metabolic disease–associated tubular damage through improving the mitochondrial energy balance. We propose that disturbances in all three major metabolic pathways (fatty acid, carbohydrate, and amino acid) can prime the development of DN/CKD, primarily through alterations in mitochondrial function, where lesions may occur first in the tubules. Our findings may also have clinical implications: provided that mitochondrial overload-induced mechanisms are the forerunners of PTC apoptosis, targeting mitochondrial function and/or energy metabolism can emerge as a new area considered for future interventions to effectively prevent, rather than treat, tubular injury and CKD.

Acknowledgments. The authors thank Dr. Katalin Susztak (University of Pennsylvania, Perelmann School of Medicine) for immensely helpful discussions and suggestions.

Funding. Research in authors' laboratories was supported by the Singapore National Medical Research Council (NMRC/OFLCG/001/2017 to J.-P.K.) and National Institute of Diabetes and Digestive and Kidney Diseases grants R01–DK-103860 (to R.C.N.), R01-DK-098687 (to R.M.), and R01-DK-115749-01A1 (to K.S.). The work used the facilities of the Cell Biology and Bioimaging Core and the Transgenics Core that are supported in part by Centers of Biomedical Research Excellence (P30-GM-118430) and Nutrition Obesity Research Centers (1P30-DK072476) grants from the National Institutes of Health.

Duality of Interest. No potential conflicts of interest relevant to this article were reported.

Author Contributions. C.K. researched and analyzed data and contributed to discussion. T.-T.N., C.B., A.G., and M.M. were responsible for maintaining the mouse colony and genotyping as well as researching data. K.T.F. and J.-P.K. conducted the mass spectrometry analyses. D.H.B. was the imaging and immunohistochemistry specialist. R.C.N. contributed to discussion and analyzed data, R.M. provided the original CrAT floxed mouse strain. K.S. supervised the experiments, designed the concept, analyzed data, and wrote the manuscript. K.S. is the guarantor of this work and, as such, had full access to all the data in the study and takes responsibility for the integrity of the data and the accuracy of the data analysis.

Prior Presentation. Parts of this study were presented as an oral presentation at Kidney Week 2015: American Society of Nephrology Annual Meeting, San Diego, CA, 3–8 November 2015.

References

1. Bonventre JV. Can we target tubular damage to prevent renal function decline in diabetes? Semin Nephrol 2012;32:452–462
2. Miltényi M, Körner A, Tulassay T, Szabó A. Tubular dysfunction in type I diabetes mellitus. Arch Dis Child 1985;60:929–931
3. Ziyadeh FN, Goldfarb S. The renal tubulointerstitium in diabetes mellitus. Kidney Int 1991;39:464–475
4. Balaban RS, Mandel LJ. Metabolic substrate utilization by rabbit proximal tubule. An NADH fluorescence study. Am J Physiol 1988;254:F407–F416
5. Elhamri M, Martin M, Ferrier B, Baverel G. Substrate uptake and utilization by the kidney of fed and starved rats in vivo. Ren Physiol Biochem 1993;16:311–324
6. Weidemann MJ, Krebs HA. The fuel of respiration of rat kidney cortex. Biochem J 1969;112:149–166
7. Schaffer JE. Lipotoxicity: when tissues overeat. Curr Opin Lipidol 2003;14:281–287
8. Listenberger LL, Han X, Lewis SE, et al. Triglyceride accumulation protects against fatty acid-induced lipotoxicity. Proc Natl Acad Sci U S A 2003;100:3077–3082
9. Sun L, Halaihel N, Zhang W, Rogers T, Levi M. Role of sterol regulatory element-binding protein 1 in regulation of renal lipid metabolism and glomerulosclerosis in diabetes mellitus. J Biol Chem 2002;277:18919–18927
10. Kang HM, Ahn SH, Choi P, et al. Defective fatty acid oxidation in renal tubular epithelial cells has a key role in kidney fibrosis development. Nat Med 2015 21:37–46
11. Stadler K, Goldberg IJ, Susztak K. The evolving understanding of the contribution of lipid metabolism to diabetic kidney disease. Curr Diab Rep 2015;15:40
12. Schelling JR. Tubular atrophy in the pathogenesis of chronic kidney disease progression. Pediatr Nephrol 2016;31:693–706
13. Susztak K, Ciccone E, McCue P, Sharma K, Böttinger EP. Multiple metabolic hits converge on CD36 as novel mediator of tubular epithelial apoptosis in diabetic nephropathy. PLoS Med 2005;2:e45
14. Schelling JR, Cleveland RP. Involvement of Fas-dependent apoptosis in renal tubular epithelial cell deletion in chronic renal failure. Kidney Int 1999;56:1313–1316
15. Wu KL, Khan S, Lakhe-Reddy S, et al. Renal tubular epithelial cell apoptosis is associated with caspase cleavage of the NHE1 Na+/H+ exchanger. Am J Physiol Renal Physiol 2003;284:F829–F839
16. Reaven GM, Hollenbeck C, Jeng CY, Wu MS, Chen YD. Measurement of plasma glucose, free fatty acid, lactate, and insulin for 24 h in patients with NIDDM. Diabetes 1988;37:1020–1024
17. Moorhead JF, Chan MK, El-Nahas M, Varghese Z. Lipid nephrotoxicity in chronic progressive glomerular and tubulo-interstitial disease. Lancet 1982;2:1309–1311

18. Ruan XZ, Varghese Z, Moorhead JF. An update on the lipid nephrotoxicity hypothesis. Nat Rev Nephrol 2009;5:713–721
19. Sas KM, Kayampilly P, Byun J, et al. Tissue-specific metabolic reprogramming drives nutrient flux in diabetic complications. JCI Insight 2016;1: e86976
20. An J, Muoio DM, Shiota M, et al. Hepatic expression of malonyl-CoA decarboxylase reverses muscle, liver and whole-animal insulin resistance. Nat Med 2004;10:268–274
21. Koves TR, Li P, An J, et al. Peroxisome proliferator-activated receptor-gamma co-activator 1alpha-mediated metabolic remodeling of skeletal myocytes mimics exercise training and reverses lipid-induced mitochondrial inefficiency. J Biol Chem 2005;280:33588–33598
22. Koves TR, Ussher JR, Noland RC, et al. Mitochondrial overload and incomplete fatty acid oxidation contribute to skeletal muscle insulin resistance. Cell Metab 2008;7:45–56
23. Muoio DM, Noland RC, Kovalik JP, et al. Muscle-specific deletion of carnitine acetyltransferase compromises glucose tolerance and metabolic flexibility. Cell Metab 2012;15:764–777
24. Kraegen EW, Cooney GJ, Turner N. Muscle insulin resistance: a case of fat overconsumption, not mitochondrial dysfunction. Proc Natl Acad Sci U S A 2008; 105:7627–7628
25. Muoio DM, Neufer PD. Lipid-induced mitochondrial stress and insulin action in muscle. Cell Metab 2012;15:595–605
26. Markwell MA, McGroarty EJ, Bieber LL, Tolbert NE. The subcellular distribution of carnitine acyltransferases in mammalian liver and kidney. A new peroxisomal enzyme. J Biol Chem 1973;248:3426–3432
27. Seiler SE, Martin OJ, Noland RC, et al. Obesity and lipid stress inhibit carnitine acetyltransferase activity. J Lipid Res 2014;55:635–644
28. Vinay P, Gougoux A, Lemieux G. Isolation of a pure suspension of rat proximal tubules. Am J Physiol 1981;241:F403–F411
29. Stevens RD, Hillman SL, Worthy S, Sanders D, Millington DS. Assay for free and total carnitine in human plasma using tandem mass spectrometry. Clin Chem 2000;46:727–729
30. Tan HC, Khoo CM, Tan MZ, et al. The effects of sleeve gastrectomy and gastric bypass on branched-chain amino acid metabolism 1 year after bariatric surgery. Obes Surg 2016;26:1830–1835
31. Nakai K, Kadiiska MB, Jiang JJ, Stadler K, Mason RP. Free radical production requires both inducible nitric oxide synthase and xanthine oxidase in LPS-treated skin. Proc Natl Acad Sci U S A 2006;103:4616–4621
32. Stadler K, Bonini MG, Dallas S, Duma D, Mason RP, Kadiiska MB. Direct evidence of iNOS-mediated in vivo free radical production and protein oxidation in acetone-induced ketosis. Am J Physiol Endocrinol Metab 2008;295:E456–E462
33. Brosius FC 3rd, Alpers CE, Bottinger EP, et al.; Animal Models of Diabetic Complications Consortium. Mouse models of diabetic nephropathy. J Am Soc Nephrol 2009;20:2503–2512
34. Wanner C, Förstner-Wanner S, Rössle C, Fürst P, Schollmeyer P, Hörl WH. Carnitine metabolism in patients with chronic renal failure: effect of L-carnitine supplementation. Kidney Int Suppl 1987;22:S132–S135
35. Gutteridge JM. Lipid peroxidation initiated by superoxide-dependent hydroxyl radicals using complexed iron and hydrogen peroxide. FEBS Lett 1984;172:245–249
36. Halliwell B, Gutteridge JM. Free radicals, lipid peroxidation, and cell damage. Lancet 1984;2:1095
37. Kanner J, German JB, Kinsella JE. Initiation of lipid peroxidation in biological systems. Crit Rev Food Sci Nutr 1987;25:317–364
38. Ruggiero C, Elks CM, Kruger C, et al. Albumin-bound fatty acids but not albumin itself alter redox balance in tubular epithelial cells and induce a peroxide-mediated redox-sensitive apoptosis. Am J Physiol Renal Physiol 2014;306:F896–F906
39. Zhu L, Jiang R, Aoudjit L, Jones N, Takano T. Activation of RhoA in podocytes induces focal segmental glomerulosclerosis. J Am Soc Nephrol 2011;22:1621–1630
40. Krall P, Canales CP, Kairath P, et al. Podocyte-specific overexpression of wild type or mutant trpc6 in mice is sufficient to cause glomerular disease. PLoS One 2010;5:e12859
41. Eremina V, Jefferson JA, Kowalewska J, et al. VEGF inhibition and renal thrombotic microangiopathy. N Engl J Med 2008;358:1129–1136
42. Seaquist ER, Goetz FC, Rich S, Barbosa J. Familial clustering of diabetic kidney disease. Evidence for genetic susceptibility to diabetic nephropathy. N Engl J Med 1989;320:1161–1165
43. Ahmad S. L-carnitine in dialysis patients. Semin Dial 2001;14:209–217
44. Noland RC, Koves TR, Seiler SE, et al. Carnitine insufficiency caused by aging and overnutrition compromises mitochondrial performance and metabolic control. J Biol Chem 2009;284:22840–22852
45. Healy MJ, Kerner J, Bieber LL. Enzymes of carnitine acylation. Is overt carnitine palmitoyltransferase of liver peroxisomal carnitine octanoyltransferase? Biochem J 1988;249:231–237
46. Bieber LL. Carnitine. Annu Rev Biochem 1988;57:261–283
47. Davies MN, Kjalarsdottir L, Thompson JW, et al. The acetyl group buffering action of carnitine acetyltransferase offsets macronutrient-induced lysine acetylation of mitochondrial proteins. Cell Rep 2016;14:243–254
48. Grgic I, Campanholle G, Bijol V, et al. Targeted proximal tubule injury triggers interstitial fibrosis and glomerulosclerosis. Kidney Int 2012;82:172–183
49. Bonventre JV. Primary proximal tubule injury leads to epithelial cell cycle arrest, fibrosis, vascular rarefaction, and glomerulosclerosis. Kidney Int Suppl (2011) 2014;4:39–44
50. Bonventre JV. Maladaptive proximal tubule repair: cell cycle arrest. Nephron Clin Pract 2014;127:61–64
51. Chevalier RL, Forbes MS. Generation and evolution of atubular glomeruli in the progression of renal disorders. J Am Soc Nephrol 2008;19:197–206